Options for CMIS C-Band RFI Mitigation: Analysis of Potential Improvements in Radiance Estimation and Soil Moisture Retrieval

J. F. Galantowicz, A. E. Lipton, and S.-A. Boukabara
Atmospheric and Environmental Research, Inc. (AER)
131 Hartwell Avenue
Lexington, MA 02421-3126
johng@aer.com

***Abstract*-The NPOESS CMIS program carried out a study in 2003 to evaluate the potential of a range of design options for improving radiometric measurements and geophysical retrievals in the presence of C-band RFI. CMIS is now in its final design phase and the results of the study are currently being applied to the final design. In this paper we present the analyses of radiance estimation and soil moisture retrieval performance used to evaluate the potential of each design option to mitigate the impact of RFI on measurements of natural earth scenes. Using an instrument and 2-D scene simulation testbed, we examined several prescribed designs incorporating subbanding, temporal subsampling, frequency shifts, and combined approaches. We describe RFI detection and mitigation algorithms developed for 4-, 6-, and 32-subband design options. Using test scenes composed from simulated natural radiances and distributed RFI emitter spectral data drawn from the JSC (Joint Spectrum Center) database, we describe performance results for the CMIS baseline single-band design and the proposed alternatives. The results show that the 32-subband design can be used to most successfully measure natural radiances and retrieve soil moisture even though it spans the spectral range most contaminated in the emitter data. The 4-subband design has comparable success but with the benefit of sampling portions of the spectrum that are currently less contaminated. We discuss the implications of this analysis under the assumption that the RFI environment will continue to worsen up to CMIS launch in 2010 and beyond.**

I. Introduction

The May 2002 launch of the Advanced Microwave Scanning Radiometer (AMSR-E) developed by the National Space Development Agency of Japan (NASDA) aboard the NASA EOS Aqua satellite brought a new awareness of the problem of RFI contamination for microwave radiometry. Simple spectral and spatial analyses of AMSR-E data show that large-magnitude (>5 K) unnatural C-band brightness temperature perturbations are widespread over the United States [1] and several other areas of the world. Furthermore, the extent of radio-frequency interference (RFI) has apparently grown considerably since the SMMR mission ended in 1987, especially within the United States.

RFI detection options for AMSR-E data are limited to 7 to 10 GHz spectral comparisons such as the RFI Index, RIp = TB7p – TB10p [1]. The RFI Index can only successfully identify RFI where it causes the total C-band brightness temperature to exceed the expected natural range relative to 10 GHz. For some surface media where 7 GHz may already be naturally larger than 10 GHz (e.g., ice and snow) the RI cannot be used. And where it is useful, it provides no practical recourse other than to drop (or accept with degraded quality) the affected 6 GHz observation from any subsequent retrieval algorithm.

In order to develop a comprehensive solution for C-band RFI detection and mitigation, Northrop Grumman Space Technology (NGST)—the prime contractor for NPOESS (National Polar-orbiting Operational Environmental Satellite System)—initiated a study in 2003 to evaluate several design options for the NPOESS CMIS (Conical-scanning Microwave Imager/Sounder) instrument. Boeing Satellite Systems (BSS) is the CMIS builder and designed the RFI mitigation hardware. Atmospheric and Environmental Research (AER) is the CMIS algorithm lead and lead the simulated performance assessments reported here, with Remote Sensing Systems (RSS) conducting the sea surface temperature (SST) retrieval tests. Since CMIS is in the final design and risk-reduction phase leading up to a critical design review in late 2005, the options considered were restricted to those judged to have a chance of accommodation within the space, mass, and power constraints of an already complex and mature design and to have acceptable risk for success in an operational program.

In this report, we present the results of end-to-end simulations of RFI mitigation option performance for brightness temperature measurement and environmental data record (EDR) retrieval (namely, soil moisture and SST). To simulate RFI spectra that were independent of the mitigation design, we used three geo-located emitter databases produced by the Aerospace Corp. from sources registered in the Joint Spectrum Center (JSC) database. The mitigation options are compared for their ability to detect and mitigation RFI, their overall impact on EDR retrievals in RFI and non-RFI environments, and their potential for success as the RFI environment worsens in the future.

II. Baseline CMIS Sensor and Operations

The baseline CMIS V- and H-pol. C-band channels (Table I) have a 350 MHz bandwidth like AMSR-E but are at a center frequency of 6.625 GHz whereas AMSR-E's is 6.925. The band was primarily designed to meet the CMIS requirements for soil moisture (SM) and SST retrieval per the CMIS Sensor Requirements Document [2] with the lower frequency range selected to avoid known emitters around 6.9 GHz. The CMIS ATBDs [3] provides more detail on the baseline CMIS design, the algorithms, and predicted retrieval performance for all 20 EDRs to be produced operationally. RFI was recognized in the initial design phase as an important component of the soil moisture retrieval error budget, and simulation tests showed that brightness temperature perturbations greater than 5 K would degrade soil moisture retrieval error to unacceptable levels. Nevertheless, RFI was assumed to be rarely occurring enough

not to impact performance on a regional or global scale and mitigation options were not pursued.

CMIS channels are positioned at four earth incidence angles and on two synchronized reflectors and many channels will not be co-registered during a given instrument scan-cycle. To maximize spectral brightness temperature co-registration and areal sampling, the CMIS algorithm suite includes a footprint-matching module that creates composite brightness temperatures from weighted sets of neighboring sensor samples [3]. Our evaluation of RFI mitigation therefore extends to the composite brightness temperatures that are used in EDR processing.

III. RFI Mitigation Designs and Algorithm

Table I lists the characteristics of the baseline design and most of the RFI mitigation options considered in the study. (Additional options with temporal subsampling are discussed briefly below.) All the options rely on the presence of one or more frequency slices that are RFI-free in a given observation cell. The multi-subband designs have the ability to detect RFI and reject contaminated subbands. The single subband tunable receiver (TUNE) is intended only to avoid the most contaminated portion of the spectrum. The dual wide-band designs (6+7 and FFT2) were selected to provide a lower frequency and lower noise band best for SST retrieval plus a RFI-avoiding (6+7 option) or RFI-mitigating (FFT2) band suitable for soil moisture retrieval in the presence of RFI.

The RFI mitigation algorithm with multiple subbands is similar to that proposed by Gasiewski et al. [4] for a 4-subband radiometer. The algorithm (a) fits a line by least absolute deviations (LAD) to brightness temperatures from N subbands and (b) calculates the median value. (LAD had higher RFI sensitivity and lower false positives than least squares.) Detection occurs if any of the absolute residuals of the fitted line exceed a tunable threshold AND any of the residuals to the median exceed the threshold. Detection also occurs if the fitted line slope exceeds a tunable threshold (10 K/GHz). Upon detection, the algorithm removes the largest-valued subband and line fitting is repeated. Detection for the 2-subband case reduces to a simple difference-threshold test.

The options were evaluated based on both RFI mitigation skill and low receiver noise. The channel NEDT of each option—the effective noise including all subbands—depends on both the net bandwidth and design differences (e.g., insertion loss) needed to accommodate the hardware. The algorithm NEDT includes any reduction in net bandwidth due to false-positive subband RFI detection by the mitigation algorithm. False-positive detection both increases the net NEDT through reduction in the usable bandwidth as well as producing a net negative brightness temperature (TB) bias due to the fact that only subbands with positive noise realizations are subject to removal by the algorithm. In addition to tuning the detection threshold to minimize false positive detection rates, the algorithm performs a post-detection bias correction when three or more subbands remain. With the correction, the largest net bias was –0.02 K.

The mitigation algorithm estimates the brightness temperature at the nominal center frequency (f_c) of each option and in simulation the TB error is evaluated with respect to the true TB(f_c). In practice, the individual remaining subband TBs may be preserved and used separately in the retrieval algorithms at their respective frequencies. We expect to adopt that approach in future algorithm development.

IV. Retrievals in RFI-Free Environments

Table I includes statistics for SST and soil moisture retrieval errors estimated for each option in RFI-free environments. (Because of on-going design changes and special test conditions used during the study, the error levels are not consistent with current CMIS performance predictions.) The TUNE option yields the most significant error degradation since both SST precision and soil moisture RMS errors increase with increasing NEDT and center frequency. We consider even small changes in the SST precision significant due to tight requirements placed on CMIS SST error performance. Lower effective NEDTs and error improvements could be gained for multi-subband options by skipping the mitigation algorithm where RFI is know to be absent (e.g., over open ocean).

V. RFI Mitigation Tests

Three RFI Scenario databases were provided by Aerospace for RFI mitigation testing. The databases contain 1000-3900 continuous-wave (CW) emitters and up to 11 pulsed emitters each spread over ~1000 km square regions. Each CW source was described by a power spectral density (PSD) in 1 MHz bins over 6400-7600 MHz. The maximum PSD of all the CW sources in RFI Scenario 2 (Fig. 1) shows that sources are found throughout the band, but the individual sources tend to be narrow-band and on a pixel-by-pixel basis the spectrum is

TABLE I
RFI Mitigation Option Summary

Mitigation Option	Frequency Span [GHz]	No. SB	SB BW [MHz]	Net BW [MHz]	SB NEDT [K]	Channel NEDT [K]	Post-Detect Algorithm NEDT [K]	False Positive Rate [%]	No-RFI SST Precision [K]	SM RMSE [%]	
										No-RFI*	w/RFI*
0. Base6	6.45-6.8	1	-	350	-	0.402	-	-	0.49	6.0	12.1
1. FFT	6.47-6.87	32	12.5	400	2.152	0.380	0.386	0.8	0.49	6.0	4.2
2a. 4SB	6.45-7.5	4	116.7	466.8	0.768	0.384	0.398	0.5	0.50	6.1	4.7
2b. 6SB	6.45-7.5	6	70	420	0.983	0.402	0.418	0.7	0.51	6.1	4.2
5a. TUNE	7.15-7.5	1	-	350	-	0.474	-	-	0.55	6.3	5.3
5b1. 6+7	6.35-6.7	1	-	350	-	0.409	-	-	0.49	-	-
	7.1-7.3	1	-	400	-	0.388	-	0.7	-	6.2	5.4
5b2. FFT2	6.35-6.7	1	-	350	-	0.409	-	-	0.51	-	-
	7.1-7.3	32	12.5	400	2.474	0.437	0.444	0.8	-	6.3	4.3

Base6=baseline design; FFT=Fast Fourier Transform; SB=subband; TUNE=tunable receiver (presumed frequency span after tuning); 6+7=dual broadband channels; FFT2=dual broadband with 32-subband FFT on upper band; NEDT is for 300 K scene brightness temperature. *SM root-mean-square-error with RFI is reported for synthetic scene with less stressing range of conditions than "no-RFI" tests.

much less contaminated. The ΔTB impact in each subband of each option for each pixel was computed primarily using the antenna gain-weighted PSD for each pixel combining all sources in the sensor footprint and the subband bandwidth.

Fig. 1: RFI Scenario 2 maximum RFI emitter spectrum.

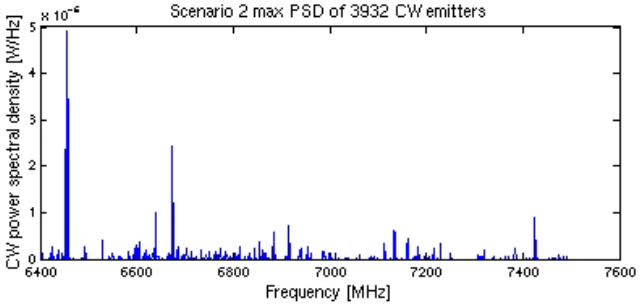

Each pulsed source was described by a pulse width, pulse repetition frequency, chirp bandwidth, and equivalent isotropic radiative power. The emitters were narrow band and high-power with many above 10^{-3} W/Hz. To avoid pulsed emitter RFI, additional mitigation options were tested with 4 or 8 temporal subsamples per 5 ms total sample integration time. However, these sample rates were too closely matched to the pulsed emitters repetition rates to provide any benefit over subbanding. Furthermore it was concluded after the study that the assumption of isotropic emitter radiation was inconsistent with the narrow beams expected from these types of emitters and that in practice pulsed-emitter RFI would rarely be encountered at the levels being simulated. Therefore, the results presented here exclude the pulsed emitters but the conclusions are consistent with those drawn with pulsed emitters nonetheless.

Two analysis approaches were used to evaluate the mitigation options against the RFI Scenario scenes. The first derived both residual RFI (in terms ΔTB) and net NEDT per composite TB observation of a simulated CMIS swath over the scene with a static 300 K natural background. These statistics were then matched to soil moisture retrieval error statistics representative of the global-annual natural environment that were tabulated in separate testbed experiments by sensor noise and ΔTB. Detection rates depend on scene brightness (which increases NEDT) and spectral slopes, so in a second approach we synthsized a natural scene with soil moisture, vegetation water content (VWC), temperature, and other environmental parameters varying on a 3 km scale. This approach provided confirmation of RFI mitigation skill over a range of specific conditions but did not provide globally representative soil moisture error statistics as the static scene did.

A. RFI Mitigation Results for Brightness temperature

Fig. 2 shows the rates of residual RFI (ΔTB) for each mitigation option. With limited ability to detect RFI, results for the baseline and TUNE options simply reveal the distribution of RFI levels within their respective bands. (We only compare the options based on in-band RFI detection; other detection methods—e.g., using 10 GHz TBs —were assumed to be significantly less sensitive than subbanding although they would be useful as a secondary screen for all of the options described here.) The two wide bands of the 6+7 option have marginal detection capabilities and so are also primarily RFI-avoiding. (The higher band is much less likely to be contaminated but where it is the lower band is likely contaminated as well.)

Fig. 2: RFI Scenario 2 rates of residual RFI.

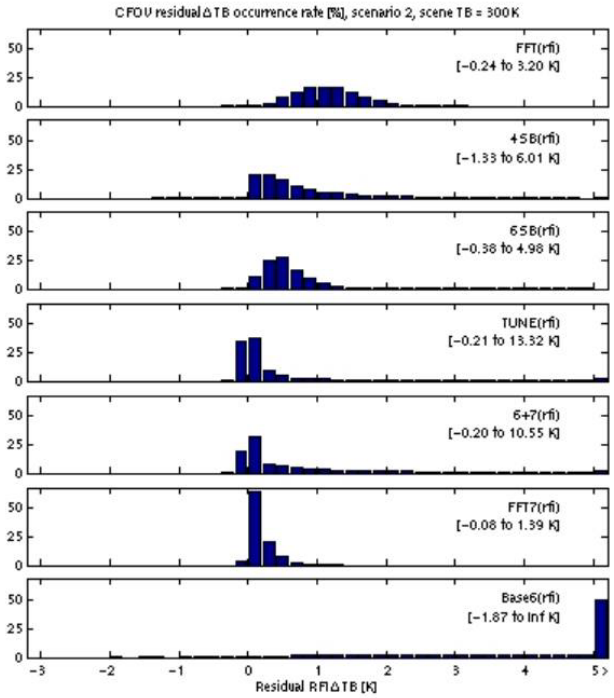

Each of the multi-subband options reduces most RFI to below the 1-2 K level. The difference between FFT and FFT2 is primarily that FFT operates in the lower band where contamination is much higher. Hence, in terms of gross RFI reduction, FFT is the most successful. The 4 and 6 subband options yield lower ΔTB levels due to a combination of detection skill and sampling of RFI-free bands.

B. RFI Mitigation Results for Soil Moisture

The CMIS algorithm derives soil moisture and VWC using 6 and 10 GHz TBs and is similar to that of Njoku and Li [5]. 6 GHz TB bias causes negative bias in the soil moisture retrieval. Fig. 3 maps the total RMS retrieval error over the RFI Scenario 2 region for the baseline and 4SB option for residual RFI levels derived from the static scene test. Large RFI-induced errors are widespread in the baseline map. White areas indicate where total TB>340 K were flagged as bad data. Most of the 4SB map has little or no RFI-induced error. The ring-shaped features are centered on RFI hot spots. In the centers, RFI is high enough to be easily detected, and farther out RFI falls to the noise level. Along the ring RFI is high enough to perturb the retrieval yet too low to be detected above the sensor noise.

Fig. 4 shows the soil moisture map of the synthetic natural scene and the retrieval bias due to RFI for the 4SB and FFT options. (The baseline bias map is similar to that in Fig. 3.) The 3 km prescribed soil moisture is smoothed by ~68x50 km composite sensor footprint (CFOV). VWC of 0, 0.5, and 1 kg/m^2 was prescribed in three ~425 km wide vertical strips. Both the 4 SB and FFT options successfully retrieve low-bias soil moisture over almost the whole scene. The FFT bias increases slightly from left to right with increasing VWC, probably as a consequence of increased algorithm

dependence on 10 GHz as net 6 GHz sensor noise levels increase with RFI detection and subband deletion. In Fig. 2 4SB has a more skewed ΔTB distribution and this translates in Fig. 4 into a larger area of near-zero soil moisture bias than FFT but more areas where the bias is large.

Fig. 3: Baseline (top) and 4SB soil moisture error maps.

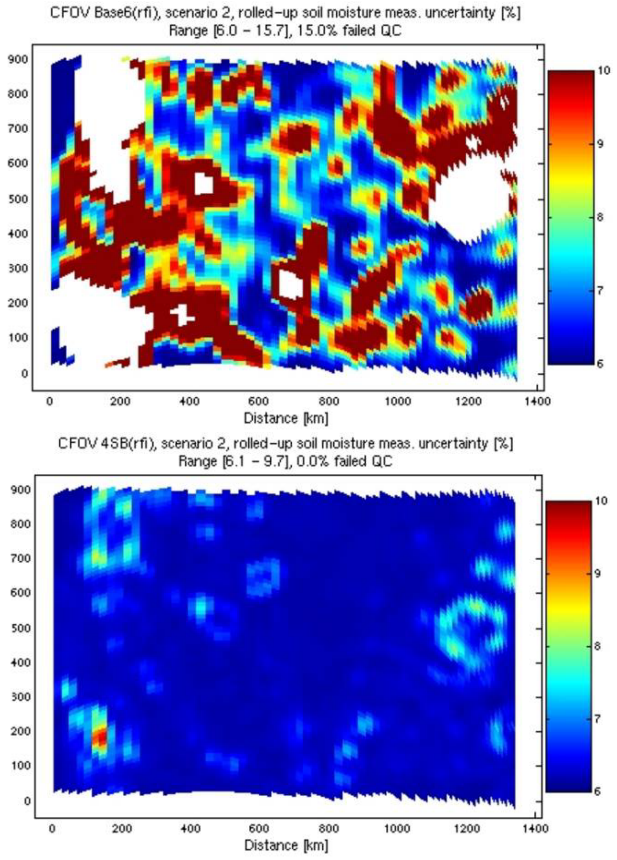

VI. Conclusion

Of the RFI mitigation options examined, FFT and 4SB had the best overall mitigation skill, reducing RFI to low levels in all three RFI Scenarios with and without pulsed emitters. Also, the FFT option was successful despite operating in the most contaminated band. The tunable receiver (higher-frequency band) avoided most RFI but is higher-risk since it has no detection skill and the presence of RFI in the 7+ GHz band suggests that future increases in contamination can be expected there. The 6+7 option is also highly at risk for increases in RFI. The FFT and 4SB options are preferable based on low-noise considerations for SST retrieval. If the RFI environment continues worsen, the high spectral resolution approach of the FFT would be best able to succeed. However, all of the techniques considered will fail if emitters are able to fill all the gaps now available for earth observation.

References

[1] L. Li, E. G. Njoku, E. Im, P. S. Chang, K. S. Germain, "A preliminary survey of radio-frequency interference over the U.S. in Aqua AMSR-E Data," *IEEE Trans. Geosci. Rem. Sens.,* 42(2):380-390, 2004.

[2] NPOESS IPO, *CMIS Sensor Requirements Document for NPOESS Spacecraft and Sensors*, 2001, http://www.npoess.noaa.gov/Library/cmis_NDX.html.

[3] J .L. Moncet et al., *ATBD for the CMIS EDRs*, AER, Inc., Vols. 1-17, 2001, http://www.npoess.noaa.gov/Library/ATBD_index.html.

[4] A. J. Gasiewski, M. Klein, A. Yevgrafov, and V. Leuskiy, "Interference mitigation in passive microwave radiometry," *IGARSS'02,* Toronto, 3:1682-1684, 2002.

[5] E. G. Njoku and L. Li, "Retrieval of land surface parameters using passive microwave measurements at 6-18 GHz," *IEEE Trans. Geosci. Remote Sensing*, 37:79-93, 1999.

Fig. 4: True synthetic soil moisture and 4SB retrieval bias.